Macromolecular Knot in Good and Poor Solvents: A Monte Carlo Simulation

Huan-Quan Sun,[†] Lu Zhang,[‡] and Qi Liao*[,§]

Shengli Oilfield Co., Ltd, SINOPEC, Dongying 257015, Shandong, China, and Technical Institute of Physics and Chemistry and Beijing National Laboratory for Molecular Sciences (BNLMS), State Key Laboratory of Polymer Physics and Chemistry, Institute of Chemistry, Chinese Academy of Sciences, Beijing 100190, China

Received: March 14, 2010; Revised Manuscript Received: August 24, 2010

The probability and dimension of the simple macromolecular knots over a wide range of temperatures corresponding from good to poor solvents are investigated by Monte Carlo simulation. Macromolecular knots are modeled as rings of self-avoiding walks on a simple cubic lattice with the nearest neighbor attractions. We found that there is a minimum probability for the unknotted ring at a certain temperature. The size dependence of trivial, trefoil, and figure-eight knots on chain lengths and temperatures is presented. The simulation results for the size dependence on the knot's complication in different solvents are in good qualitative agreement with prediction of the scaling model proposed by Grosberg et al. The critical exponent for long chain is independent of the knot types based on the simulation results, although the mean square radius of gyration is influenced significantly by the knot types for a shorter length macromolecular ring. We calculated the ratio of the topological invariant p of trefoil knot and figure-eight knot and found that the ratio is approaching to 1.3 with the increasing of the chain length.

1. Introduction

The entanglement effect caused by the topological constraints in many-chain systems plays central roles in polymer dynamics.[1] However, the effect in the study of the single chain was generally not considered to be serious because the properties in dilute solutions are usually dominated by the external modes for which the topological constraints are not important.[2] This conjecture was supported by the scaling theory and the results of computer simulation; both indicated that the topological constraints affect only the numerical factor,[2,3] but with the rapid development of molecular biology in recent years, it is found that the topological properties of a single biological macromolecule are of great importance in the study of protein folding,[4,5] gel electrophoresis of circular DNA,[6,7] as well as DNA recombination and replication.[8,9] Although the single macromolecular knot could be observed under electron microscopy[10] and tied with the optical tweezers,[11] its statistic properties are extremely difficult to describe because of the lack of powerful theoretical tools.

To date, the main theoretical results to estimate the size of macromolecular knots come from the method of scaling analysis. Quake first presented a simple phenomenological theory to estimate the size of macromolecular knots with chain length, N, and the following scaling law for the radius of gyration, R_g, is obtained[12]

$$R_g \propto N^{\nu} C^{1/3-\nu} \tag{1}$$

where C is the number of essential crossing and ν is the Flory exponent. Grosberg introduced a weak topological invariant p that is the aspect ratio of the length to the diameter of a knotted macromolecule in a maximally inflated tube and presented a mean field theory of the effect of knots on the statistical mechanics of ring polymer.[13] To balance the free energy contribution of rubber-like elasticity and the volume interactions between monomers, the theory predicted that the radius of gyration R_g relates

$$R_g \propto aN^{3/5}\tau^{1/5}p^{-4/15} \quad \text{in good solvent regime} \tag{2}$$

$$R_g \propto aN^{1/2}p^{-1/6} \quad \text{in quasi-Gaussian regime} \tag{3}$$

$$R_g \propto aN^{1/3}|\tau|^{-1/3}\left[1 + |\tau|^{-4/3}\left(\frac{p}{N}\right)^{2/3}\right] \quad \text{in poor solvent regime} \tag{4}$$

where $\tau = 1 - (\theta/T)$ denotes the dimensionless deviation from the θ temperature. Comparing both theories, we can expect that there is a linear relationship between p and C for the consistency of eqs 1 and 3 in the quasi-Gaussian regime. This conclusion was also drawn by the results of previous computer simulations.[14,15]

Numerous computer simulations on the knot state of chain structure were performed in the past two decades.[16−23] These computer simulation results presented the probability of knotted polymer in collapse regime modeled as Hamilton cycles,[18] in θ state modeled as random walk,[16] and from θ state to good solvent as off-lattice rod-bead chain.[17] Even though the models mentioned above can give some statistical properties of macromolecular knots in special regime, it is difficult to describe the transition over a wide range of temperatures.

Recently, the research interests of the simulations in the field are focused on the stability of tight polymer knots,[24,25] which was first presented by de Gennes.[26] Even the knotted polymer could not lead to the long-time memory effects in the melts of crystallizable, linear polymer based on the simulation results; the relaxation time of the single chain knotting in the collapse

* To whom correspondence should be addressed. E-mail: qiliao@iccas.ac.cn.
[†] SINOPEC.
[‡] Technical Institute of Physics and Chemistry, Chinese Academy of Sciences.
[§] Beijing National Laboratory for Molecular Sciences (BNLMS), State Key Laboratory of Polymer Physics and Chemistry, Institute of Chemistry, Chinese Academy of Sciences.

10.1021/jp1023179
Published on Web 09/08/2010

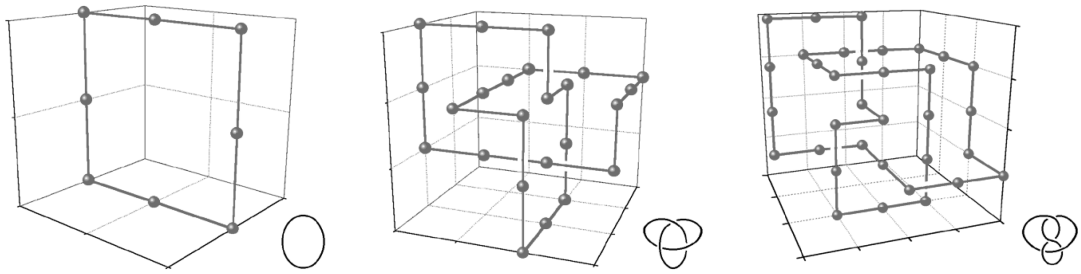

Figure 1. Three simplest knots on a cubic lattice: (a) trivial knot, (b) trefoil knot, and (c) figure-eight knot. The trefoil knot ($N = 24$) and figure-eight knot ($N = 34$) given in the Figure are the shortest knots on the simple-cubic lattice.

transition seems to be the most fundamental for both chemical and biological applications.[12,20,27]

The scaling analysis in refs 12 and 13 could give the limiting behavior of knot's size in good and poor solvents, but the information in the transition regimes and the rate of approach to the limiting behavior is little known. It is the purpose of this Article to investigate the dependence of the different temperatures on the probabilities and dimensions of some simple macromolecular knots. The rest of the Article is organized as follows. The simulation model and the algorithm are described in Section 2. Section 3 gives a detailed account of the simulation results for probability and dimension of macromolecular knot type as functions of chain length and temperature. Finally, we discuss our results and compare them with the scaling analysis results proposed by Grosberg et al.

2. Model and Algorithm

The behavior of a polymer under various solvent conditions has been modeled by self-avoiding walks (SAWs) with the nearest neighbors (NN) attraction energy ε ($\varepsilon < 0$).[28] To compare with the previous simulation results of coil−globule transition from good solvent to poor solvent, we adopted the similar scanning method of Meirovitch[28] to construct the rings of SAW on a simple cubic lattice. The method is briefly described here. The construction of a SAW ring of length N includes two pathways. First, a linear SAW of length $N/2$ is generated step-by-step with the weight W_{i1}

$$W_{i1} = \frac{1}{6}\prod_{k=2}^{N/2}\frac{l_k}{(2d-1)} \tag{5}$$

where l_k is the number of unoccupied sites at step k and d is 3 in three dimension. Then the SAW ring is closed by the following $N/2$ steps with the weight W_{i2}

$$W_{i2} = \prod_{k=N/2+1}^{N}\frac{l'_k}{(2d-1)} \tag{6}$$

where l'_k is the number of site unoccupied and feasible to return to the origin at step k.

Once a SAW ring of length N has been generated, there is a weight $W_i = W_{i1} \times W_{i2}$. The normalized probability can be obtained by $P_i = W_i/\sum W_i$. By using the biased probability, P_i, the correct statistical average $\langle V\rangle$ can be estimated from a sample of size, n

$$\langle V\rangle = \sum_{t=1}^{n} V_{it}P_{it}e^{-E_{it}/k_BT}/\sum_{t=1}^{n} P_{it}e^{-E_{it}/k_BT} \tag{7}$$

TABLE 1: Occurrence Frequencies of Three Kind Knots in the Simple Biased Sampling

length	total samples	trivial knots	trefoil knots	figure-eight knots	unknown knots
50	5 000 000	4 999 737	262	1	0
100	5 000 000	4 995 761	4152	79	8
150	5 000 000	4 987 328	12 125	460	87
200	5 000 000	4 975 300	23 294	1147	259
250	5 000 000	4 961 067	36 243	2040	650
300	5 000 000	4 943 779	51 712	3281	1228
400	5 000 000	4 907 369	82 937	6650	3044

where t is the t-th SAW generated with the scanning procedure, k_B is the Boltzmann constant, and T is the absolute temperature.

Figure 1 illustrates three simplest knots: (a) trivial, (b) trefoil, (c) and figure-eight knots, which are constructed on a simple cubic lattice. All polygonal knots have regular projection, so the constructed ring can be always projected in a proper direction. We used a 2-D projection of a knot onto a plane to determine the topological state in our calculation.

We chose the Alexander polynomial $\Delta(s)$ to identify the knot types.[17,29] If the number of crossings is too large, then it can produce very high-rank determinant, therefore making the calculation difficult. Therefore, we must simplify the ring chain before the projection transition, and a similar smoothing operation in ref 17 is used before determining the Alexander polynomial. The smoothing operation is, simply said, when there is no other bond transferring the triangle region made by $n - 1$, n, and $n + 1$ lattice sites; the n lattice site is canceled, so $n - 1$ and $n + 1$ lattice sites are connected with one bond. The number of the crossings decreases significantly in this way.

Table 1 shows the occurrence frequency of three kinds of knots in the simple biased sampling of 5 000 000. The unknown knots increase significantly when the chain is longer than 300, and the results become unreliable. Therefore, we use only the data of chain length 30−300 in our Results and Discussion section.

3. Results and Discussion

A. Determination of Good Solvents and Poor Solvents. At high temperature or in a good solvent, the short-range repulsive interaction (excluded volume interaction) is dominating among monomers, resulting in swelling of a chain whose size is larger than a random coil. At low temperature or in a poor solvent, monomer−monomer contacts become favorable, and the chain tends to collapse into a compact dense globule. At an intermediate temperature, called θ temperature, the repulsive and attractive interactions cancel each other. To determine if the chain or ring swells or collapses, we followed the method used by Meirovitch and Lim et al.[28,30,31]

Figure 2 shows the ratio of mean-square radius of gyration to the chain length ($\langle R^2\rangle/N$) versus chain length N at different

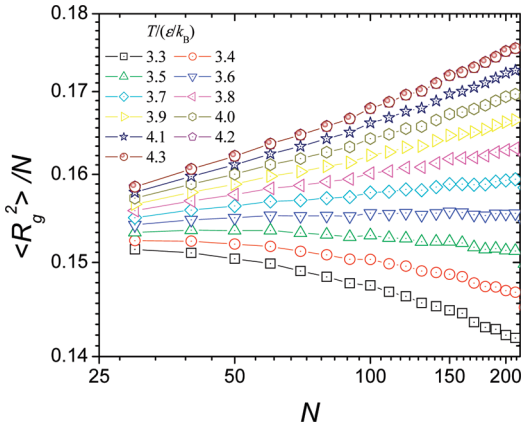

Figure 2. Log−Log plot of $(\langle R^2\rangle/N)$ versus N for the different temperature.

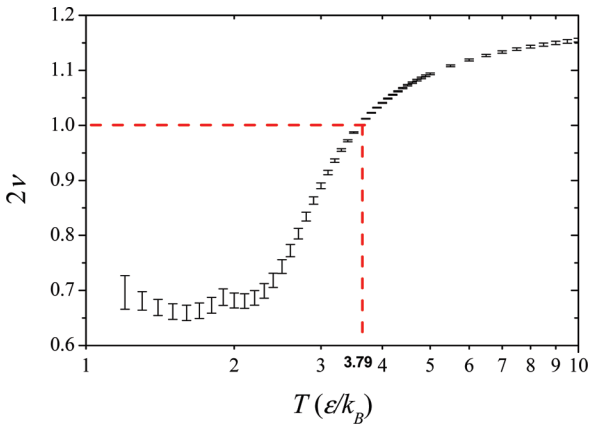

Figure 3. Critical exponent 2ν at different temperatures assuming $\langle R^2\rangle \propto N^{2\nu}$.

temperatures. Short chains will swell with an exponent $\nu < 0.588$ even in poor solvents, and the exponent increases and is approaching 0.588 when chains get longer. An opposite trend is expected in poor solvents where the mean-square radius of gyration of short chains grows with $\nu > 1/3$. The exponent decreases to 1/3 for longer chains as temperature decreases in poor solvents.

Figure 3 shows the critical exponent 2ν at different dimensionless temperatures, assuming $\langle R^2\rangle \propto N^{2\nu}$. The exponent 2ν increasing from 0.67 to 1.18 with higher temperature indicates that the macromolecular ring undergoes the transition from a compact globule to a swelling coil. The exponent ν at the temperature $3.79(\varepsilon/k_B)$ is ~0.51, which is in excellent agreements with the well-known value 1/2. We use the temperature $3.79(\varepsilon/k_B)$ as the point to estimate the properties of solvents for our simulation chains. The chain is swelled in the good solvent far above $3.79(\varepsilon/k_B)$ and is collapsed in the poor solvents far below the temperature.

B. Probability of Macromolecular Knots. We are interested in the equilibrium distribution of the rings with different knot types. In a good solvent, the swollen coils are expected to be relatively unknotted, whereas the collapsed globules are expected to be extensively knotted at the equilibrium state. The previous works of Mansfield and Koniaris, in which the system is not far below the θ temperature, supported the above conjecture. Figure 4 gives the contribution of the three simplest knot types at different temperatures. From Figure 4a, it is found surprisingly that there is a minimum probability of unknotted ring (trivial knot) at a certain temperature, which increases with the chain length. The existence of the minimum probability of unknotted

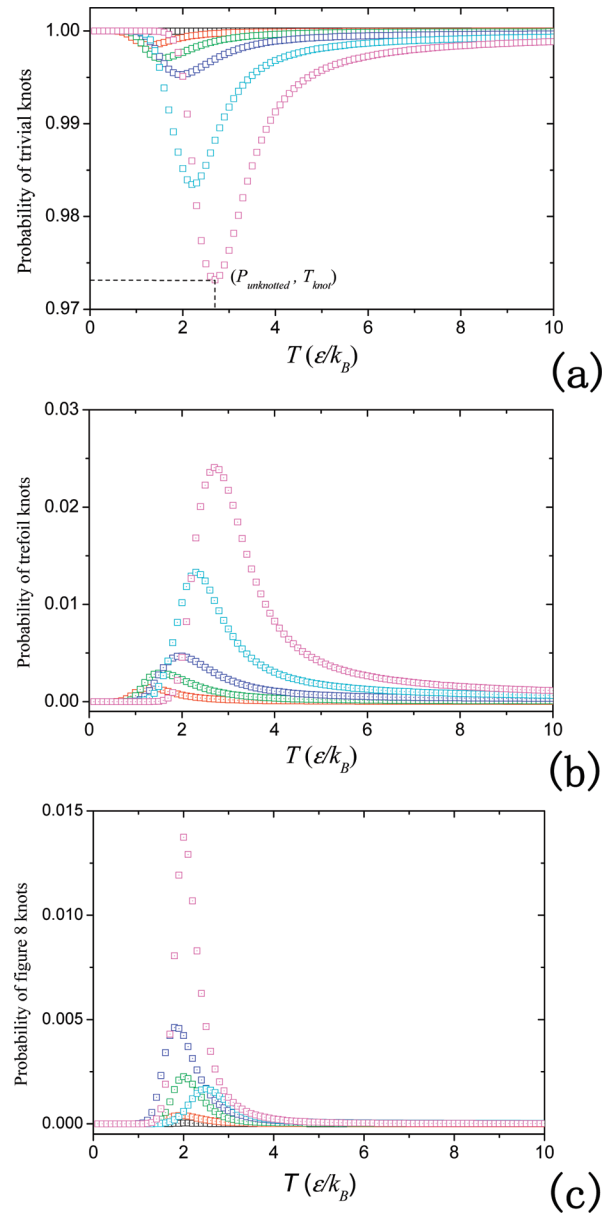

Figure 4. Probability of three knot types at different temperatures. (a) Trivial knot, length $N = 30$ (the upper line), 50, 70, 100, 150, 250 (the lower line); (b) trefoil knot, length $N = 250$ (the upper line), 150, 100, 70, 50, 30 (the lower line); (c) figure-eight knot: length $N = 200$ (the upper line), 150, 130, 170, 110, 90 (the lower line), respectively.

ring indicates that the chains tend to disentangle in the regime far below the θ temperature. We define the temperature corresponding to the minimum probability of a unknotted ring $P_{\text{unknotted}}$ as the maximum entanglement temperature for a single knot, denoted as T_{knot}.

Figure 5 shows the minimum probability $P_{\text{unknotted}}$ of unknotted ring and corresponding temperature T_{knot} at various chain lengths. The data are fitted with the following equations

$$P_{\text{unknotted}} = 1 - B\mathrm{e}^{(N-N'_0)/N'_1} \tag{8}$$

$$T_{\text{knot}} = T_{\max} - A\mathrm{e}^{-(N-N'_0)/N'_1} \tag{9}$$

The best fitting curves are shown in Figure 5, where $B = 2.07$, $N'_0 = 492$, $N'_1 = 68 \pm 14$; $T_{\max} = 2.57 \pm 0.11$, $A = 1.40 \pm 0.12$, $N_0 = 40$, $N_1 = 77 \pm 20$.

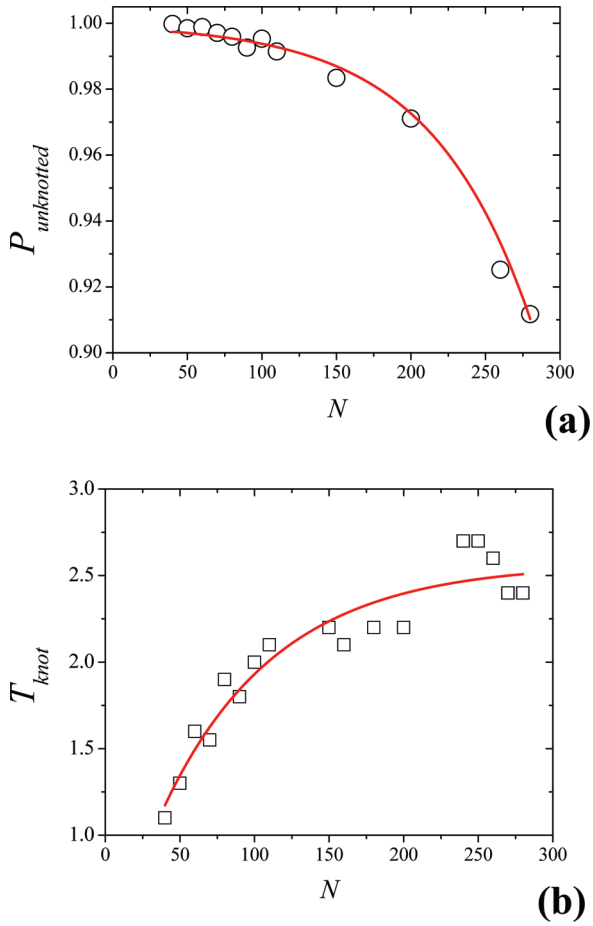

Figure 5. (a) Minimum probability of unknotted ring and (b) corresponding temperature at various chain lengths.

The fitting results show that the maximum entanglement temperature of T_{knot} is $\sim 2.57(\varepsilon/k_B)$, which is in its collapse regime in poor solvents (Figure 3). When the globule is in poor solvents, the chain segment would pack in a more ordered manner because of the lower energy, and the unknotted ring is preferred to construct the conformation. With the increase in the temperature in poor solvents, the chain would also be unknotted because of the entropy contribution of the unknotted chain. Therefore, we predict that there is a particular temperature nor far away from T_θ, at which a chain is in the most entangled state. However, the entanglement state of the chain is of equilibrium properties and may be hampered by the kinetic factor in the experimental observation.[32]

C. Dimension of Macromolecular Knots. Figure 6 shows the mean-square radius of gyration of knot rings in athermal solvent ($\varepsilon = 0$, or $T \to \infty$). The data are fitted with the equation

$$\langle R^2 \rangle = CN^{2\nu} \tag{10}$$

and the best fitting parameters are given in Table 2, where the error bars are 95% confidence intervals. Although the numerical factors C are sensitive to knot types, the critical exponents are independent of the knot types in the error range.

The intuitive expectation is that topological constraints suppress both swelling in a good solvent and collapse in a poor solvent. Figure 7 shows the mean-square radius of gyration of knot rings in various regimes for chain length $N = 200$. We observed that the more complicated the knot is, the smaller the

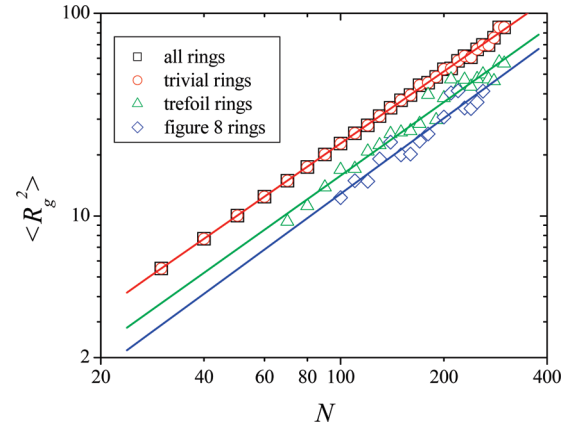

Figure 6. Mean square radius of gyration of knot rings in athermic solvent ($\varepsilon = 0$ or $T \to \infty$).

TABLE 2: Exponent 2ν and Numerical Factor C (eq 7) of Rings with Different Knot Type in Athermal Solvent ($\varepsilon = 0$ or $T \to \infty$), Where the Error Bars Are 95% Confidence Intervals

	log C	2ν
all rings	-1.00378 ± 0.015	1.1806 ± 0.007
trivial knots	-1.00375 ± 0.015	1.1807 ± 0.007
trefoil knots	-1.21 ± 0.11	1.205 ± 0.046
figure-eight knots	-1.37 ± 0.22	1.239 ± 0.097

temperature dependence of dimension is, which agrees qualitatively with the theory proposed by Grosberg et al.

Figure 8 shows the radii of gyration of different knot types at the various dimensionless deviation from the θ temperature $\tau = 1 - (\theta/T)$, and the limiting lines proposed by Grosberg et al. (eqs 2 and 4) are also shown. The simulated results are qualitatively consistent with the theory proposed by Grosberg et al in the regime of good and poor solvents. However, the mean field theory does not agree very well with our data quantitatively in these regimes except for the trivial knot ring.

To verify the mean field theory in the quasi-Gaussian regime, the ratio of topological invariance p of figure-eight and trefoil knots at various inverse chain lengths is calculated by eq 3, and the results are given in Figure 9. The dash line is $p = 1.3$ obtained from ref 14. It is found that the ratio is in agreement quite well with the topological invariance p in ref 14.

4. Conclusions

Our simulation predicted that there is a maximum entanglement temperature T_{knot} for a single chain knot. T_{knot} is below

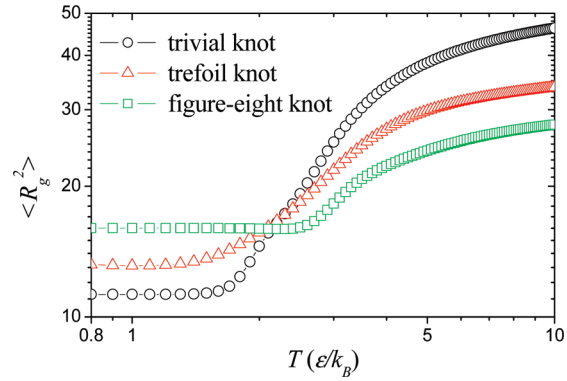

Figure 7. Mean-square radius of gyration of knot rings at various temperatures for $N = 200$.

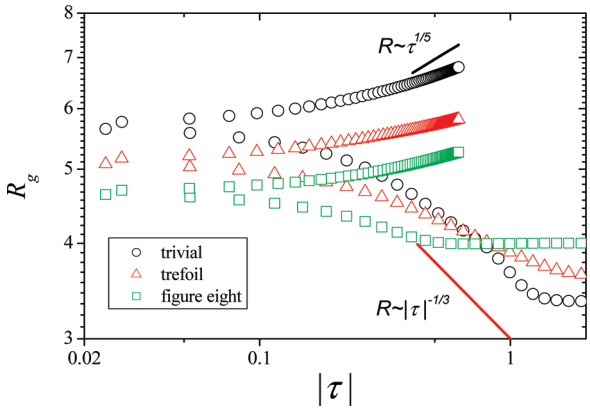

Figure 8. Radius of gyration of different knot types versus the dimensionless deviation from the temperature $\tau = 1 - (\theta/T)$. The limiting lines proposed by Grosberg et al (eqs 2 and 4) are also shown. The length $N = 200$.

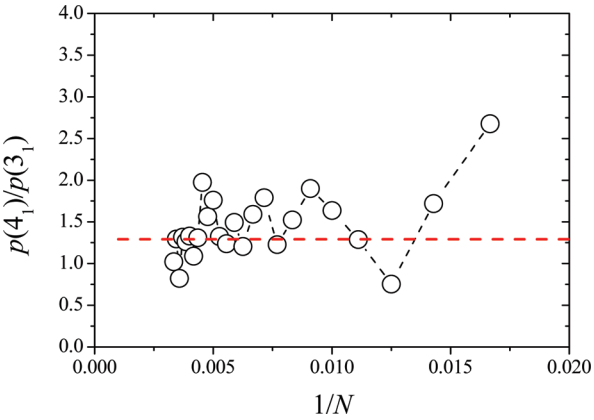

Figure 9. Ratio of topological invariant p of figure-eight knot and trefoil knot at various inverse chain lengths. The dashed line $p = 1.3$ denotes the result from ref 14. See the text for the details.

the θ temperature T_θ but not too far away from T_θ. The existence of the maximum entanglement state of a single chain could significantly affect the viscosity and diffusion properties of the macromolecules; this may have an effect on DNA and proteins in the gel electrophoresis. We hope our results of the maximum entanglement temperature presented here will motivate the experimental measure of the temperature.

In our simulation, all types of rings cross over from a compact globule to a random coil, then to a swelling coil as the temperature goes from poor solvent to good solvents. Our simulation also confirmed that there is a weaker temperature dependence of more knotted macromolecule rings.

Acknowledgment. This work was financially supported by the National Science & Technology Major Project (2008ZX05011) of China, National High Technology Research and Development Program (2008AA092801) of China, and NFSC grant no. 20974115.

References and Notes

(1) de Gennes, P. G. *Scaling Concepts in Polymer Physics*; Cornell University Press: London, U.K., 1979.
(2) Doi, M.; Edwards, S. F. *The Theory of Polymer Dynamic*; Clarendon Press: Oxford, U.K., 1986.
(3) Rensburg, E.; Whittington, S. G. *J. Phys. A: Math. Gen.* **1991**, *24*, 3935.
(4) Mansfield, M. L. *Nat. Struct. Biol.* **1997**, *4*, 166.
(5) Baker, D. *Nature* **2000**, *405*, 39.
(6) Zeman, S. M.; Depew, K. M.; Danishefsky, S. J.; Crothers, D. M. *Proc. Natl. Acad. Sci. U.S.A.* **1998**, *95*, 4327.
(7) Vologodskii, A. *Proc. Natl. Acad. Sci. U.S.A.* **1998**, *95*, 4093.
(8) Wasserman, S. A.; Cozzarelli, N. R. *Science* **1986**, *232*, 951.
(9) Wasserman, S. A.; Cozzarelli, N. R. *Science* **1985**, *229*, 171.
(10) Krasnow, M. A. *Nature* **1983**, *304*, 559.
(11) Arai, Y.; Yasuda, R.; Akashi, K.; Harada, Y.; Miyata, H.; Kinosita, K.; Itoh, H. *Nature* **1999**, *399*, 446.
(12) Quake, S. R. *Phys. Rev. Lett.* **1994**, *73*, 3317.
(13) Grosberg, A. Yu.; Feigel, A.; Rabin, Y. *Phys. Rev. E* **1996**, *54*, 6618.
(14) Katritch, V.; Bednar, J.; Michoud, D.; Scharein, R. G.; Dubochet, J.; Stasiak, A. *Nature* **1996**, *384*, 142.
(15) Katritch, V.; Olson, W. K.; Pleranski, P.; Dubochet, J.; Stasiak, A. *Nature* **1997**, *388*, 148.
(16) Brinke, G. T.; Hadziioannou, G. *Macromolecules* **1987**, *20*, 480.
(17) Koniaris, K.; Muthukumar, M. *J. Chem. Phys.* **1991**, *95*, 2873.
(18) Mansfield, M. L. *Macromolecules* **1994**, *27*, 5926.
(19) Fawcett, A. H.; Mee, R. A. W.; McBride, F. V. *J. Chem. Phys.* **1996**, *104*, 1743.
(20) Sheng, Y.; Lai, P.; Tsao, H. *Phys. Rev. E* **1998**, *58*, R1222.
(21) Guitter, E.; Orlandini, E. *J. Phys. A: Math. Gen.* **1999**, *32*, 1359.
(22) Sheng, Y.; Liao, C. *J. Chem. Phys.* **2003**, *118*, 4748.
(23) Orlandini, E.; Stella, A. L.; Vanderzande, C. *Phys. Rev. E.* **2003**, *68*, 031804.
(24) Mansfield, M. L. *Macromolecules* **1998**, *31*, 4030.
(25) Saitta, A. M.; Soper, P. D.; Wasserman, E.; Klein, M. L. *Nature* **1999**, *399*, 46.
(26) de Gennes, P. G. *Macromolecules* **1984**, *17*, 703.
(27) Grosberg, A. Yu.; Kuznetsov, D. V. *Macromolecules* **1993**, *26*, 4249.
(28) Meirovitch, H.; Lim, H. A. *J. Chem. Phys.* **1990**, *92*, 5144.
(29) Crowell, R. H.; Fox, R. H. *Introduction to Knot Theory*; Spring-Verlag: New York, 1977.
(30) Rubio, A. M.; Freire, J. J.; Bisshop, M.; Clarke, J. H. R. *Macromolecules* **1995**, *28*, 2240.
(31) Wittkop, M.; Kreitmeler, S.; Goritz, D. *J. Chem. Phys.* **1996**, *104*, 3373.
(32) Grosberg, A. Yu.; Kuznetsov, D. V. *Macromolecules* **1993**, *26*, 4249.

JP1023179